Revista Colombiana de Física, Vol. 43, No. 2 de 2011.

Espartaco: A High-Resolution, Low-Cost Spectrograph For Students

Espartaco: Un Espectrógrafo Didáctico De Alta Resolución Y Bajo Costo

B. Oostra [*a], D. Ramírez [a]

[a] *Universidad de los Andes, Bogotá, Colombia.*

Recibido 17.04.10; Aceptado 18.12.10; Publicado en línea 04.09.11.

Resumen

Reportamos la construcción de un espectrógrafo de alta resolución y bajo costo, comisionado para mediciones astronómicas y físicas en la Universidad de los Andes en Bogotá. El instrumento es alimentado mediante fibra óptica desde el telescopio o desde cualquier otro montaje. Para objetos suficientemente luminosos se puede alcanzar una resolución de 105. Con el telescopio actual se obtienen espectros útiles de estrellas de primera magnitud en 10 minutos de exposición, a una resolución de 27000. Mediciones de corrimiento espectral presentan una incertidumbre de 10-7 cuando la relación de señal a ruido es suficientemente alta. El nombre ESPARTACO significa "Espectrógrafo de Alta Resolución para Trabajos Astronómicos en Colombia".

Palabras clave: Astronomía; Espectrografía; Instrumentación.

Abstract

We report the construction of a high-resolution, low-cost spectrograph for astronomical and physical observations at the Universidad de los Andes in Bogotá. The instrument is fed by means of an optical fiber from the telescope or from any other equipment. A resolution of 105 can be attained for sufficiently luminous objects. With the presently available telescope facilities, useful spectra of first-magnitude stars are obtained with exposures of 10 minutes, at a resolution of 27000. Redshift measurements exhibit an uncertainty around 10-7 when the S/N ratio is sufficiently high. The nickname ESPARTACO stands for "Espectrógrafo de Alta Resolución para Trabajos Astronómicos en Colombia".

Keywords: Astronomy; Spectrography; Instrumentation.

PACS: 95.55.-n.

1. Introduction

Astronomical measurements are not only a craving of star enthusiasts, but also a welcome alternative to physics students in search of an experimental project. The atmospheric conditions at our campus severely limit the possibility of precise astronomical observations, except for spectroscopic measurements, a fact that has prompted the development of several spectrographs at this Observatory. Our previous design has proven useful for spectral classification of stars [1] and analysis of bright HII-regions like the Orion nebula; that instrument attained a resolution of $R = \lambda/\Delta\lambda \approx 6000$, but, being attached directly to the telescope, lacked the desired mechanical stability for accurate velocity measurements. A comparable instrument called BACHES [2], developed at ESO (European Southern Observatory), though giving higher resolution (19000) by means of an Echelle grating (which works in high orders, $N \approx 100$), accused similar deformations as the telescope moved. Our choice toward more stability was a fiber-coupled spectrograph. Shelyak Instruments has commercialized a tabletop fiber-coupled Echelle spectrograph, with seemingly negligible mechanical problems and a reported resolution of 12000 [3]; our instrument, however,

* boostra@uniandes.edu.co

offers greater resolution due to its greater focal length. An amateur spectrograph of similar characteristics has been reported by Kaye et al. [4].

2. Requirements

Our first two major considerations while planning ESPARTACO were high resolution and mechanical stability, in order to improve the Doppler measurements and spectral line separation given by our previous equipment. Next, the instrument had to be low-cost, because our turbulent and light-polluted atmosphere does not justify great investments in astronomical equipment. Another important goal has been that the instrument should be easy to operate and very reliable, because, particularly for astronomy, good observing time is scarce and cannot be wasted in tinkering with the apparatus. In addition, a last important factor considered for design: Our observatory is small, and the instrument should occupy little floor area.

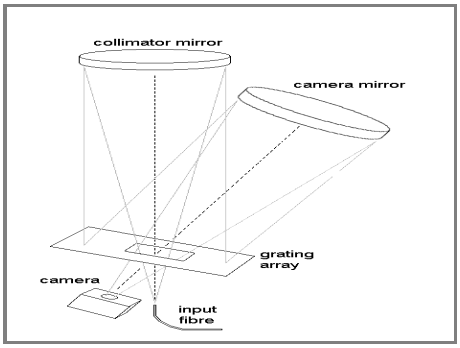

Fig. 1: Schematic view of the optics.

3. Optical layout

The general arrangement can be seen in Figure 1. The "X" design is due, in part, to the lack of physical space at our observatory.

We use reflection-type diffraction gratings working in first order. The instrument has place for a total of eight 50-mm-square gratings. The presently installed gratings have densities of 1200 and 2400 lines/mm. The gratings are arranged around a central aperture that allows light to come from the fiber and go to the camera. Each grating is independently adjusted for vertical and horizontal position of the spectrum, and additionally rotated to trace the spectra parallel to the camera axis.

The collimator and camera use parabolic mirrors: The collimator has 17 cm diameter and a focal length of 127 cm; the camera is wider, with 20 cm diameter and 91 cm length.

Two fibers feed the light directly into the collimator, without a slit. One has 50 μm diameter and the other 10 μm; both images fall simultaneously onto the camera, so that either can be used as an absolute wavelength reference for spectra taken with the other. The 50 μm fiber gives slightly broader spectral lines, meaning less resolution, but far more luminous spectra. These fibers are not only a convenient way for bridging the distance from the telescope to the spectrograph; they are also handy probes in all kind of optical experiments.

The CCD camera spans 1530 by 1020 pixels, the size of each pixel being 9 μm square. The spectra are aligned with the longer camera axis. Depending on which grating is used, spectra are 50 or 100 Angstrom long. The chip temperature is maintained typically at -10°C by a Peltier element plus air-cooling.

The only movable part is the grating assembly; to choose the required wavelength, this module is manually rotated by means of a precision knob and a 5:1 reduction. Any desired portion of the optical spectrum can be centered on the image with a precision of a few Angstrom. This does not make the instrument a spectrometer, but for a spectrograph, it has turned out to be very user-friendly.

4. Review of basic theory

The basic equation describing the behavior of a reflective diffraction grating is:

$$\sin(i) + \sin(r) = \frac{n\,\lambda}{d} \tag{1}$$

Here i and r represent the incidence and reflection angle, and d is the groove spacing. The two angles are of the same sign when located at the same side of the grating normal. If ψ represents the position angle of the grating, measured from the bisector between the two arms of the spectrograph, we have the following equivalences:

$$i = \psi + \delta\,, \qquad r = \psi - \delta\,. \tag{2}$$

The angle δ is half the angle between the collimator and the camera. From here we obtain a convenient relation between the grating position and the observed wavelength:

$$\sin(\psi) = \frac{n\,\lambda}{2\,d\,\cos(\delta)}\,. \tag{3}$$

From equation 1 we obtain the dispersion in pixels per Angstrom, leaving i fixed and allowing r to vary over the width of the camera; we include the camera focal length f and pixel size p:

$$\frac{dx}{d\lambda} = \frac{n\,f}{p\,d\,\cos(r)}\,. \tag{4}$$

We now calculate the theoretical resolution: A rectangular slit of width W subtends a small Δi; the corresponding Δr is obtained from equation 1 for a fixed λ. The projected slit image in the camera has a width w given by

$$w = W \frac{f \cos(i)}{F \cos(r)}, \quad (5)$$

where F and f are respectively the collimator and camera focal lengths. Here we see that the choice $i > r$ gives a narrower image and a consequently greater resolution. Combining this result with Equation 4, we find the wavelength range subtended by the projected slit image:

$$\Delta\lambda = \frac{W\ d \cos(i)}{n\ F}. \quad (6)$$

Remarkably, the resolution is independent of the camera focal length. The length of the camera must be chosen in such a way that the projected slit width covers a few pixels. The theoretical minimum is 2 pixels, a value known as Nyquist's sampling frequency [5]: An image smaller than 2 pixels implies a loss of information, but a much greater image spreads the light over an unnecessarily extended area, lowering the S/N ratio and calling for longer exposures.

The numerical resolution is defined as:

$$R = \frac{\lambda}{\Delta\lambda}. \quad (7)$$

In astronomical measurements, R values of a few tens of thousands are (still) regarded as "high resolution".

Although our spectrograph has a circular fiber aperture instead of a rectangular slit, this formula gives a reasonable approximation to the practical resolution. Our collimator has F = 1271 mm. Substituting the 50 μm fiber diameter for the "slit width", using the 2400 grooves/mm grating, and choosing ψ = 50° which gives i = 58° and λ = 6300 Angstrom, we get a theoretical resolution of R = 72500, a value which is only about 10% higher than experimental results.

5. Some construction details

The main frame of the 2 m high instrument was built from 5 cm wide steel angle. Surrounding this, a wooden box serves for protection, separated from the steel frame by an air gap and Styrofoam sheets, providing mechanical and thermal insulation. This construction favors also a dark internal environment, but long exposures demand still better optical insulation, which is supplied by a black rubber bag inside the structure, surrounding the optical elements.

The two mirrors were obtained from Dobsonian amateur telescopes. The camera is a model ST-1603ME from SBIG (Santa Barbara Instruments Group). The diffraction gratings were purchased from Edmund Optics. Optical fibers and further supplies are locally available at low costs.

Quite a few alignment screws have been included in the design, but not for all degrees of freedom; the alignment of the camera with the grating rotation axis was performed using a detachable lever, and a similar procedure was performed for the alignment of each grating with the camera.

For the obtention of stellar spectra the optical fiber must be attached to the telescope in such a way that the selected star can be found, focused, and centered on the fiber; additionally the telescope's sky tracking must be monitored. We have achieved this by embedding the fiber in the centre of a slightly tilted mirror, mounted at the eyepiece-end of the telescope. A small off-axis CCD camera captures the image, so that the whole procedure may be conducted from a computer.

6. Initial results

The 1200 grating gives a dispersion of about 15 pixels per Angstrom in a first-order spectrum at 6300 Angstrom; the 2400 grating gives 33 pixels per Angstrom.

Experimentally, a spectral line, which is a monochromatic image of the slit or fiber, has not a rectangular intensity profile, but rather a Gaussian-like profile. Measuring its width at half-maximum intensity, the 50 μm fiber gives about 3.5 pixels of line width, if properly focused. Combining these results, the 2400 grating yields a resolution of about 65000. Fig. 2 shows such a spectrum, although the resolution is somewhat lower due to non-optimal focusing.

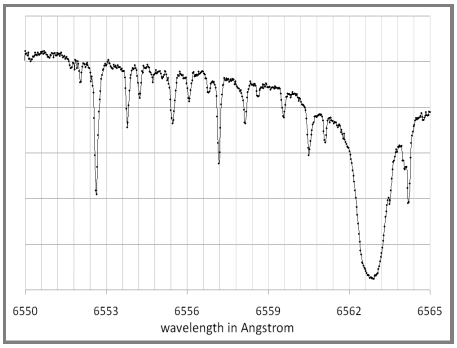

Fig. 2: A portion of the solar spectrum. Absorption lines are about 4 pixels wide, and R = 56000. The broad line is H-alpha; most of the narrow lines are due to water vapor in the Earth's atmosphere.

The 10 μm fiber can produce a profile width of 2 pixels, giving a resolution of 1×10^5; but this fiber can only be

used for very bright objects, because the smaller diameter cuts down the throughput by a factor of 25; this poses, however, no difficulty for the study of emission spectra from discharge tubes, because in this case the light is not distributed over a long continuous spectrum, but rather concentrated in relatively few spectral lines, giving sufficiently bright images in most cases.

For stars, the only useful configuration is the 50 μm fiber with the 1200 grating; this combination gives a resolution of about 27000; an exposure of 10 minutes produces a useful spectrum of a first-magnitude star, with an S/N ratio of 60. From there on, each higher magnitude will need about three times that exposure.

On solar spectra using the 2400 grating, positions of spectral lines can be measured with an uncertainty of a few mili-Angstrom. This gives an uncertainty of about 100 m/s for Doppler measurements with a single line. This uncertainty may be even as low as 50 m/s when the S/N ratio is high and an ensemble of lines can be measured on a single spectrum.

7. Wavelength calibration

For Doppler measurements, spectral lines must be identified in order to know their natural wavelengths; and further, the spectrum's observed wavelengths must be known, for which purpose a calibration process must be carried out. With ESPARTACO, there are three methods of wavelength calibration which can be used:

1. A calibration spectrum may be included in the same image as the object spectrum, through the other fiber.
2. Atmospheric absorption or emission lines may be present in the object spectrum and can be used for calibration.
3. Several independent calibration spectra may be taken before and/or after the object spectrum.

Each of these methods has some advantages and disadvantages: As for the first method, it is very convenient to have the calibration spectrum and the object spectrum in one single image; it is easier to handle just one image and know that everything is there; moreover, you do not have to worry about possible instrument shifts between consecutive images. However, bright emission lines may be scarce in some wavelength ranges, depending on the available sources; and many lines are needed for a good calibration. Moreover, the calibration spectrum is not located on the same pixel row as the object spectrum, but shifted vertically by hundreds of rows, making it necessary to project one spectrum onto the other. This projection should correct a horizontal shift of some 20 pixels; the exact shift, which must be known for the calibration, is not a constant number: it depends on the grating angle and also on the horizontal position on the image; these dependences should be carefully assessed, but they will always introduce some uncertainty; at present, this uncertainty is of the order of 0.05 pixel.

Atmospheric lines may be very useful for calibration because they are included in the object spectrum with no need of projection; neither do they suffer from instrumental shifts between consecutive images. Nevertheless, they are not always available wherever they are needed. Water vapor lines, for example, are to be found abundantly over the whole visible spectrum; but at night they disappear, at least on our observing site, due to condensation. Oxygen lines, though available around the clock, are limited to a few wavelength bands; for example, a few dozen of them are to be found around 5300 Angstrom. We have performed calibrations of solar spectra using these oxygen lines, finding an overall statistical uncertainty of 0.01 pixels.

The method of independent calibration spectra has the advantage of using the same fiber as the object spectrum, avoiding projection errors; moreover, it is possible to take several such spectra, making it possible to assess their repeatability; one may even average them to get a more trustworthy calibration; but if fluctuations are large, there remains a considerable uncertainty about the actual calibration of the object spectrum. This method demands the instrument to be free of time-varying mechanical or geometrical deformations, a quality referred to as mechanical stability.

8. Test of stability

In order to test the mechanical stability of the instrument, we took 100 identical spectra at regular intervals and compared them. The spectra were taken from a neon tube through the 50 μm fiber. Each exposure lasted 2 seconds and an interval of 30 seconds was allowed between exposures, so the duration of the whole experiment exceeded 50 minutes, longer than any typical observation. Three emission lines appear on each spectrum, the well-known neon lines at 6507, 6533, and 6599 Angstrom, which are located close to H-alpha. A routine was written on the MIDAS software package [6] to measure the positions and widths of the 300 images in both dimensions.

The first evident result is that the positions are not constant; they increase about half a pixel during the test, as shown in Fig.3. Initially the line positions increase linearly with time, besides a dispersion of 0.027 pixels. After 20 minutes, they stabilize around a constant mean position, but with a greater dispersion (0.061 pixels). This behavior reflects the temperature evolution of the CCD detector.

The thermal variation depends on the work rate of the camera and the temperature set point. The camera includes a temperature sensor which shows only discrete steps of about 0,4°C, making it difficult to monitor the variation precisely. Moreover, the CCD chip is never at a single temperature, and anisotropy effects are not negligible. This problem is quite unavoidable, but can be minimized by a suitable setting of the temperature control and a proper stabilization time.

The line widths are not constant, as may be seen in Fig. 4; initially they decrease to a minimum, which occurs about halfway the test, and then increase again. This reflects the instability of the focusing mechanism. The fact that the optimum focus of horizontal profile is attained during the experiment is no chance, but responds to the careful, manual horizontal focusing previous to the test. Vertical focusing is observed to be farther from optimal, giving clear evidence of some astigmatism; but this is of minor importance, because spectra are usually extracted by adding several horizontal pixel lines. The focus instability may be solved or controlled by future mechanical improvement of the instrument.

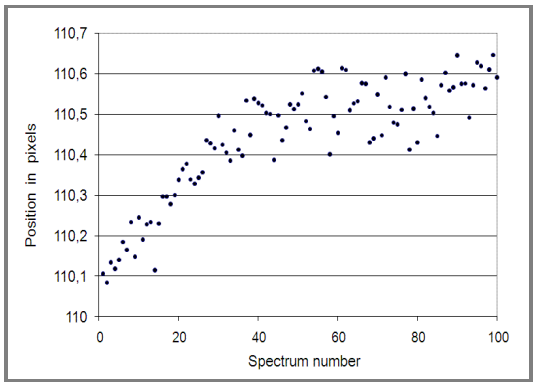

Fig. 3: Horizontal positions of a spectral line in 100 consecutive identical spectra. Note the initial increase and subsequent stabilization, as well as the dispersion around this trend.

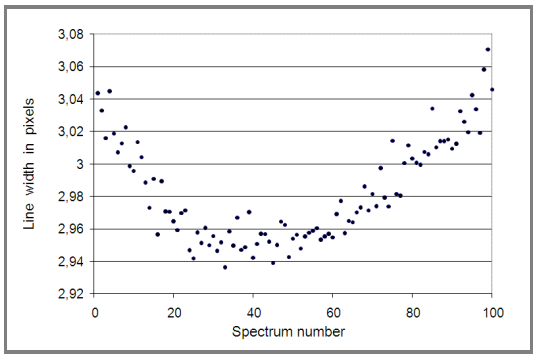

Fig.4: Horizontal widths of a spectral line in 100 consecutive identical spectra. Note the minimum halfway the experiment, when the focus may be considered as optimal.

9. Conclusion

ESPARTACO provides a valuable opportunity for students to embark on interesting observation projects. Possible topics include binary stars, radial oscillations of variable stars, rotation of the Sun, translation and rotation of the Earth, extrasolar planets, chemical abundance measurements, spectral classification of stars, and monitoring of emission lines in Be-type stars. Besides astronomy, the instrument allows accurate measurements of the Doppler effect, Zeeman effect and atomic fine structure.

Most of our users are physics students in laboratory or astronomy courses. In addition, external users such as high school students or astronomy clubs are welcome. Our main goal is to provide these students with an opportunity to get acquainted with the techniques of observational physics and astronomy, so that they can learn hands-on to take their own spectra, reduce the images, calibrate and analyze the data and interpret the results.

The quality of the instrument answers to our expectations. Wavelength calibrations exhibit uncertainties of a few hundredths of a pixel, which translate to a velocity margin of 100 m/s or less.

The use of this instrument presents, however, several difficulties. First of all, continuous spectra are modulated by intensity oscillations, as may be seen in Fig. 5; in the worst cases, this modulation completely drowns the absorption lines. The effect is probably due to intermodal interference in the fibers [7], and can be partially avoided making the incidence of the light onto the fiber as isotropic as possible; solar spectra are almost completely free of modulation if the fiber is not pointed directly at the Sun but at some diffuse source of sunlight, like bright clouds or a white wall, at the expense of requiring longer exposure times.

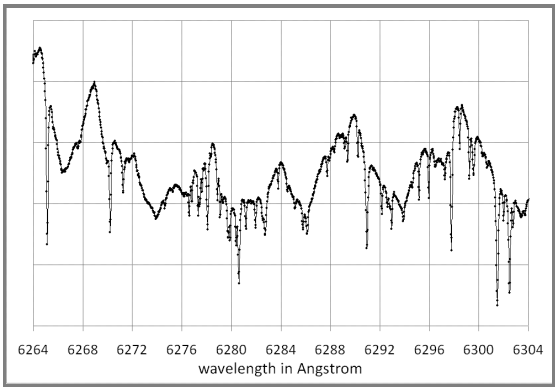

Fig. 5: A portion of the solar spectrum, showing strong modulation of the continuum.

Another technical difficulty is the failure of the spectrograph to remain in focus for a long time, and the necessary refocusing when switching to another grating.

A third drawback is the obviously low throughput with the ensuing long exposures; a partial solution to this may be the use of less dense gratings, which would lower the resolution, but also the exposure time, while conveniently increasing the number of lines in each spectrum; but anyhow, the use of ESPARTACO for stellar astronomy seems to be restricted to the brightest stars in the sky.

10. Acknowledgements

This project is supported by the Departamento de Física and the Facultad de Ciencias of the Universidad de los Andes at Bogotá.

We thank Professor Gabriel Téllez for drawing our attention to Hlubina's articles.

References

[1] Ramírez, David. Clasificación espectral de estrellas. Bogotá, 2005, 38 h. Trabajo de grado (Físico). Universidad de los Andes. Facultad de Ciencias. Departamento de Física.

[2] Ávila, Gerardo; Burwitz, Vadim; Guirao, Carlos; Rodríguez, Jesús; Shida, Raquel; Baade, Dietrich. BACHES – a compact light-weight echelle spectrograph for amateur astronomy. In: The Messenger, No. 129 (Sept. 2007), pp. 62-64. ISSN 0722-6691. Online available at: <http://esoads.eso.org /abs/2007Msngr.129...62A>

[3] Buil, Christian. The observation of Tau Bootis exoplanet with the eShel spectrograph [online]. <http://astrosurf.com/buil/tauboo/exoplanet.htm> [referenced March 1, 2010].

[4] Kaye, Tom; Vanaverbeke, Sigfried; Innis, John. High-precision radial-velocity measurement with a small telescope: Detecting the Tau Bootis extrasolar planet. In: Journal of the British Astronomical Association, Vol. 116, No. 2 (2006), pp. 78-83. ISSN 0007-0297. Online available at: <http://arxiv.org/abs/astro-ph/0609468v1>

[5] Gray, David. The Observation and Analysis of Stellar Atmospheres. Third edition. Cambridge, Cambridge University Press, 2005. 533 p. ISBN 978-0-521-85186-2.

[6] European Southern Observatory. ESO-MIDAS [online]. http://www.eso.org/sci/data-processing/ software/esomidas/ [referenced April 16, 2010].

[7] Hlubina, Petr. Measuring dispersion between two modes of an optical fiber using low-coherence spectral interferometry with a Michelson interferometer. In: Journal of Modern Optics, Vol. 46, No. 11 (1999), pp. 1595-1604. ISSN 0950-0340.